



HAL
open science

The origin of high hydraulic resistance for filter cakes of deformable particles: cell-bed deformation or surface-layer effect?

Martine Meireles, Catherine Molle, Michael J. Clifton, Pierre Aimar

► To cite this version:

Martine Meireles, Catherine Molle, Michael J. Clifton, Pierre Aimar. The origin of high hydraulic resistance for filter cakes of deformable particles: cell-bed deformation or surface-layer effect?. *Chemical Engineering Science*, 2004, 59 (24), pp.5819-5829. 10.1016/j.ces.2004.06.040 . hal-00323043

HAL Id: hal-00323043

<https://hal.science/hal-00323043>

Submitted on 22 Sep 2008

HAL is a multi-disciplinary open access archive for the deposit and dissemination of scientific research documents, whether they are published or not. The documents may come from teaching and research institutions in France or abroad, or from public or private research centers.

L'archive ouverte pluridisciplinaire **HAL**, est destinée au dépôt et à la diffusion de documents scientifiques de niveau recherche, publiés ou non, émanant des établissements d'enseignement et de recherche français ou étrangers, des laboratoires publics ou privés.

The origin of high hydraulic resistance for filter cakes of deformable particles: cell-bed deformation or surface-layer effect?

M. Meireles*, C. Molle, M.J. Clifton, P. Aimar

Laboratoire de Génie Chimique (CNRS UMR 5503), Université Paul Sabatier,

118 Route de Narbonne, 31062 Toulouse cedex, France

Abstract

This study reports a numerical approach for modeling the hydraulic resistance of a filter cake of deformable cells. First, a mechanical and osmotic model that describes the volume fraction of solids in a bed of yeast cells as a function of the compressive pressure it experiences is presented. The effects of pressure on the compressibility of yeast cells beds were further investigated both by filtration experiments and by centrifugal experiments based on the multiple speed equilibrium sediment height technique. When comparing the latter measurements with compression model calculations, we observed that the method based on centrifugal experiments suffers from rapid relaxation of the compressed bed. Concerning the filtration experiments,

* Corresponding author. Tel. +33 561 55 8162; fax: +33 561 88 6139
E-mail address: meireles@chimie.ups-tlse.fr (M. Meireles)

specific resistance of well defined bed of cells were calculated by a combination of the compression model with a formulation for hydraulic resistivity developed using the Lattice Boltzmann method. We further explain the experimental values observed for the hydraulic resistance of cell beds, assuming that the first layer of cells in contact with the membrane partially blocks the membrane area open to flow. In such a case, the blocked area seems to be a constant fraction of the normal cell-cell contact area.

Keywords:

4 recommended : filtration, porous media, soft solids, downstream processing

2 others: hydraulic resistance, Lattice Boltzmann

1. Introduction

Microfiltration is an economical and efficient technique for separating, from a liquid medium, particles ranging from one tenth of a micrometer up to a few micrometers in size. This technique is used for concentrating slurries in the food, beverage and cosmetic industries and for separation of cells in the biotechnology industry. Although this method is widely used to separate deformable or soft particles in such various chemical and biochemical processes, the factors that affect the filtration rate such as hydrodynamics, surface chemistry at particle surfaces and compressibility of cakes or particles are still not well understood or documented and significant error in the estimation of filtration rate occurs when conventional filtration theory is applied.

The cake that builds up on the membrane surface plays a major role in operating performance as it controls the transient flux decline. This latter is usually approximated by dead-end filtration theory (Redkar & Davis, 1993), with the rate of flux decline correlated to the amount deposited via the hydraulic resistance associated with the cake buildup.

A large number of papers have been published that report the hydraulic resistance of filter cakes formed from biological suspensions such as microbial suspensions, yeast suspensions or red-blood-cell suspensions. Rushton & Khoo (1977), Ofsthun (1989), Nakanishi, Tadokoro & Matsuno (1987), Nomura (1989), Piron, René & Latrille (1995), Ogden & Davis (1990) have all measured the hydraulic resistance of deposits of baker's yeast (*Saccharomyces cerevisiae*). Collected data vary in a finite range where variations can be ascribed to the differences in particle size, state of agglomeration, age, pH of liquors or the concentration of extra-cellular compounds.

Despite these differences, much useful knowledge can be acquired by examining results from all these different studies carried out with the same type of suspension. Fig. 1 gathers together some of these data for the specific resistance of baker's yeast filtered in the pressure range 0 - 400 kPa. We have also compared these data with values calculated using the traditional Carman-Kozeny equation assuming Stokes flow through a granular bed of 5 μm diameter particles (which is close to the mean diameter for yeast particles) and a void fraction of 0.27 corresponding to the maximum packing of a face-centered cubic array. As illustrated in Fig. 1, the experimental cake resistances for yeast are more than a hundred times higher than the values predicted. Experimental values also show a pressure dependence which is not accounted for by this simple equation.

Most authors invoke the compressible nature of biological cells to explain the discrepancy between Carman-Kozeny predictions and experimental data, the calculated value being the lower limit when no compressive pressure is applied to the bed (Piron, René & Latrille, 1995).

Indeed, developments in filtration theory have aimed at providing detailed descriptions of fluid motion through a filter cake due to a pressure gradient. This gradient causes an interfacial momentum transfer in the form of a viscous drag at the particle-fluid interfaces. If the shape or strength of the particles is such that the packing arrangement cannot sustain this drag without further movement occurring then the cake is regarded as compressible. The modeling approaches involved to describe the influence of cake compressibility on flow properties and volume fraction gradient in the cake have been well described in several papers, for example Tiller (1975), Shirato, Murase & Iwata (1986), Tiller, Yeh & Leu (1987), Sorensen, Moldrup & Hansen (1996).

If the compressible nature of many cakes is recognized in most of these works, the physical description of the forces acting on the packing re-arrangement is still not really understood nor described. For the case of biological cells, two mechanisms can count as major sources of the increase in hydraulic resistance with pressure: an increase in area-contact between the particles due to deformation or re-orientation by frictional drag , and formation of a compact skin layer next to the membrane surface due to the mass of particles.

This article is concerned with the physical interpretation of the values of specific resistance measured during filtration experiments of yeast suspensions for different operating pressures.

This study treats the following points:

- experimental observation of the behavior of yeast suspensions (model suspensions) under compressive loads
- development of a realistic model for the mechanical properties of a bed of yeast cells and their impact on its hydraulic resistance for low porosity, with incorporation of a modified Carman-Kozeny equation, established by the Lattice Boltzmann method,
- integration of this model into an overall filtration model and comparison with the experimental results
- discussion of the relative importance of cake and surface-layer contributions in controlling the hydraulic resistance.

2. Theoretical development

The model developed here has a certain similarity with a two-dimensional model for red blood cells proposed by Zydney, Saltzman & Colton (1989). They assumed that

the cells could be represented by hexagonally packed discs with cell deformation by flattening in the regions of cell-cell contact. This deformation was further assumed to occur by stretching of the cell membrane at constant cell volume. In the present case, a three-dimensional structure is assumed and deformation involves not only stretching of the membrane but also osmotic equilibrium.

2.1. *Geometry of cells as a function of mechanical load and osmotic stress*

In a series of recent publications, Smith, Moxham & Middelberg (1998, 2000) and Smith, Zhang & Thomas (2000) studied the mechanical properties of yeast cells. A slightly simplified version of their model is used here with the aim of providing a realistic description of the compressive deformation of yeast in the filter cake; the content of this model is briefly presented in Eqs.(1) to (8). These authors found that the cell membrane is sufficiently permeable for an isolated cell to reach osmotic equilibrium in about 5 s. As we are interested in long-term behavior of the filter cake, we assume here that the cells are continually in osmotic equilibrium: $\Delta p - \Delta \Pi = 0$, where $\Delta p = p_c - p_l$ is the turgor pressure, i.e. the pressure difference between the cell interior and the surrounding liquid. This can be written as:

$$\Delta p + \Pi_l - \Pi_c = 0 \quad (1)$$

If the osmotic pressure outside the cells Π_l is increased, their volume diminishes and the situation is finally reached where Δp is abolished, i.e. the cell membrane is no longer under tension and then we have: $\Pi_{c0} = \Pi_{l0}$. According to Smith, Zhang & Thomas (2000), the value of Π_{c0} is 2.1 MPa. Under these conditions, the cell volume is V_{c0} , its surface area S_{c0} and r_0 (2.51 μm) is the radius of a sphere having the same volume and surface area.

A common hypothesis, also adopted by Smith, Zhang & Thomas (2000), is that the osmotic pressure inside the cells follows a form of the van't Hoff equation:

$$\Pi_c(V_c - V_n) = \Pi_{c0}(V_{c0} - V_n) \quad (2)$$

Here V_n is a non-osmotic volume, which is an important fraction of the volume V_{c0} : $V_n = \beta V_{c0}$ and $\beta = 0.65$ according to Smith, Zhang & Thomas (2000).

By combining these equations, it is possible to obtain a relationship giving the cell volume that is fixed by the osmotic equilibrium:

$$V_c = V_{c0} \left(\beta + \Pi_{c0} \frac{1 - \beta}{\Delta p + \Pi_l} \right) \quad (3)$$

On the other hand, the cell membrane is considered as extensible. The relationship between the tension T of the membrane (assumed isotropic), the turgor pressure and the radius of curvature r is given by the Laplace equation:

$$\Delta p = \frac{2T}{r} \quad (4)$$

The membrane is assumed to be perfectly elastic, so the tension is proportional to the surface deformation:

$$T = K \frac{S_c - S_{c0}}{S_{c0}} \quad (5)$$

Here K is the surface modulus, whose value was determined by Smith, Zhang & Thomas (2000) to be 11.4 N m^{-1} . Though these authors also studied a three-dimensional model of the cell membrane, we restrict our treatment here to the two-dimensional version and neglect any tension produced by membrane shear and flexion.

In this way it is possible to arrive at a relationship for the surface area of the cell as it is fixed by the elastic stretching of the membrane:

$$S_c = S_{c0} \left(1 + \frac{r \Delta p}{2K} \right) \quad (6)$$

Before considering the compressed cells, it is important to determine the internal pressure of a non-compressed spherical cell of radius r . We define the ratio $\lambda = r/r_0$. As $V_c/V_{c0} = \lambda^3$ Eq. 3 can be put into the form:

$$\Delta p' = \Pi_{c0} \frac{1 - \beta}{\lambda^3 - \beta} - \Pi_l \quad (7)$$

Also as $S_c/S_{c0} = \lambda^2$ Eq. 6 becomes:

$$\Delta p' = \frac{2K}{\lambda r_0} (\lambda^2 - 1) \quad (8)$$

The value of λ is determined so that the two Eqs. 7 and 8 give the same turgor pressure $\Delta p' = p'_c - p_l$, corresponding to the value for non-compressed cells.

We assume that in the case of compressed cells the total internal pressure is the sum of this initial pressure and the compressive pressure p_s :

$$p_c = p'_c + p_s \quad (9)$$

The geometry of the compressed cells is then established by considering that the cells have a roughly spherical form, are of uniform size and are arranged in face-centered cubic packing. We assumed that under a compressive load, the surface of contact between two cells will no longer be spherical but flat, while the untouched part of the cell retains a spherical shape: one can also think of the cells as represented by overlapping or interpenetrating spheres.

To calculate the surface area and volume fraction of these cells we consider a spherical envelope from which segments are removed and replaced by flat areas: each

sphere has 12 neighbors and will ‘lose’ 12 segments. If the distance between the centers of two neighboring cells is $2a$ and r is the radius of curvature, then r/a can be thought of as a *stretch ratio*: it is equal to 1 for non-deformed cells and increases with increasing deformation. The volume of each cell V_c is related to this ratio in the following manner:

$$V_c = \frac{4}{3}\pi a^3 \left[9\left(\frac{r}{a}\right)^2 - 5\left(\frac{r}{a}\right)^3 - 3 \right] \quad (10)$$

The surface area of each cell is found in a similar way:

$$S_c = 4\pi a^2 \left[6\frac{r}{a} - 2\left(\frac{r}{a}\right)^2 - 3 \right] \quad (11)$$

Face-centred cubic packing can be represented by a repeating cube of side $2a\sqrt{2}$ that contains the volume of 4 cells. So the volume fraction of cells in this compressed packing is related to the stretch ratio as follows:

$$\phi = \frac{\pi}{\sqrt{2}} \left[3\left(\frac{r}{a}\right)^2 - \frac{5}{3}\left(\frac{r}{a}\right)^3 - 1 \right] \quad (12)$$

In the same way, the liquid-solid interface area per unit volume can be calculated:

$$S = \frac{\pi}{a\sqrt{2}} \left[6\frac{r}{a} - 5\left(\frac{r}{a}\right)^2 \right] \quad (13)$$

This geometry remains permeable for values of r/a at which the ‘triangular’ openings remain open: $1 \leq r/a < 2/\sqrt{3}$.

It is worth noting that the model of Smith, Zhang & Thomas (2000) contains four parameters Π_{c0} , r_0 , β and K that were determined by these authors. Though their

measurements did not claim to reach a high accuracy, we have used their values in the rest of this work.

2.2. Hydraulic resistivity of a porous medium at low porosity

Even though cell membranes are found to be moderately permeable, the cells will be taken as constituting an impermeable solid phase. The hydraulic resistivity of this porous medium can be represented using the Carman-Kozeny equation:

$$r_h = K_0(\phi) \frac{S^2}{(1-\phi)^3} \quad (14)$$

It is known that at high volume fraction ϕ the value of K_0 increases strongly with ϕ (Dullien, 1979) and it is quite inaccurate to use the traditional value for a bed of spherical particles. The hydraulic resistivity of this porous geometry was calculated by the Lattice Boltzmann method (Succi, 2001). This numerical technique for calculating flow patterns is particularly well adapted to the complex geometries that are found in porous media. For this calculation, the 3-dimensional image of the pore structure was a cube, 104 voxels in length. Periodic boundary conditions were imposed on all opposing faces, with a pressure jump between the two faces on the flow direction. It was found that the results of this numerical calculation could be represented by a simple function in which the Kozeny coefficient K_0 varies with ϕ in the following way (Meyeres, Clifton & Aymar, 2002):

$$K_0 = \left[a_0 + \frac{a_1}{\phi_{lim} - \phi} \right] \quad (15)$$

Here ϕ_{lim} is the volume fraction of solid phase for which the narrowest openings between cells are closed, so that the cake resistance tends towards infinity.

Fig. 2 is a flow diagram showing how Equations 3 and 6 – 15 can be used to determine r_h and ϕ as a function of p_s . The numbers in the diagram are the equation numbers and the presence of several numbers in a single block indicates a simultaneous solution; the values in the upper left-hand corner are parameters of the problem (yeast properties and the osmotic pressure of the filtrate). Because of the non-linearity of the system of equations a direct calculation is not possible: instead the ratio r/a is varied over the range of possible values (from 1 up to a value for which the structure is almost closed) and this allows calculation of ϕ , r_h and p_s . These values are tabulated and in subsequent calculations spline interpolations are used to calculate ϕ and r_h from p_s .

2.3. *Model for permeation*

The model for the mechanics of cell deformation and its effect on hydraulic resistivity has been incorporated into a permeation model that applies Darcy's law:

$$\frac{dp_l}{dx} = -r_h \langle u \rangle \eta \quad (16)$$

Here p_l is the liquid pressure, x is the distance in the flow direction, r_h is the hydraulic resistivity, $\langle u \rangle$ is the superficial velocity of the liquid (an imposed value) and η its viscosity.

On the basis of a force balance, the drop in liquid pressure is usually considered to be compensated by an increase in the compressive pressure in the solid:

$$p_0 = p_s + p_l \quad (17)$$

The hydraulic resistivity is a function of the compressive pressure, which is related to the liquid pressure by Eq. 17.

The specific resistance of the cake α is calculated according to the equation:

$$\langle u \rangle = \frac{p_0}{\eta(R_m + \alpha m)} \quad (18)$$

The specific resistance is related to the mass of “solids” in the cake (including the water in the cells). The mass m of filter cake per unit membrane area is given by the integral:

$$m = \int_0^{X_d} \rho_c \phi dx / A \quad (19)$$

This integration is performed numerically simultaneously with the resolution of Eq. 16 taking account of Eq. 17 and of the variation of r_h and of ϕ with p_s .

The limiting conditions for Eq. 16 are as follows: at the upper surface of the cake, at $x = 0$, p_l is equal to the filtration pressure p_0 and at the cake-membrane interface, at $x = X_d$, $p_l = \langle u \rangle \eta R_m$. Here R_m is the effective hydraulic resistance of the membrane and X_d , the cake thickness determined by integrating Eq. (16) for increasing x values until the experimental value for the mass of filter cake is reached.

3. Materials and methods

3.1. Yeast suspensions

Suspensions of baker’s yeast *Saccharomyces Cerevisiae* were prepared from commercially available Active Dry Yeast (Lessaffre) which were suspended in isotonic saline water (8 g/L NaCl, pH = 6.0). During the rehydration process, soluble compounds can be released in the suspension. Rehydrated suspensions are thus centrifuged at 4000 rpm for 15 minutes at 20°C (Centrikon T-124, Kontron

Instruments). The sediment is then collected and resuspended in isotonic saline water. This operation is repeated three times in order to remove the released soluble species. The final sediment is then collected and resuspended in isotonic saline water. The final solution, designed as “washed solution”, free from soluble compounds is then constituted from yeast cells suspended in saline water. The density of washed rehydrated yeast cells ρ_c is equal to 1130 kg/m³.

Yeast cells are ovoid particles: their mean particle diameter was determined using a Disk Centrifuge Particle Analyzer (Brookhaven Instruments Corporation, USA). A mean diameter of $5 \pm 3 \mu\text{m}$ was found. Observations with an optical microscope (Axiolab A- Reflected Light Microscope, Zeiss, Germany) revealed that “washed” cells are close to spherical particles, the size distribution observed being the result of some daughter cells present at the surface of a few yeast cells. Observations also confirm that using the washing procedure, all the cell debris had been removed.

3.2. *Filtration experiments and determination of specific resistance*

For a given hydrostatic pressure, we measured the specific resistance of filtration cakes of a well defined mass. This was done by monitoring the permeate volume over time during filtration of the suspension and by measuring the flux at steady state with an isotonic saline solution.

The experimental set-up consists of a pressurized reservoir (Amicon), a 0 - 600 kPa pressure gauge (AGA) and a dead-end unstirred cell (Amicon 8050, Millipore) which is a cylindrical vessel with a porous bottom plate acting as a membrane support. We used a 0.1 μm acetate microfiltration membrane, 13.4 cm² in area (Orelis, Saint Maurice de Beynost, France). Pressure was set in the range 30 - 300 kPa by means of

compressed air and permeate mass was recorded on an electronic balance (Precisa 1600 C – Oerlikon – 5/1600 g).

A yeast suspension of known volume and initial concentration (1 g/L or 20 % v/v) was placed in the filtration cell and saline solution was continuously fed from the reservoir to the cell under constant pressure. The suspension then forms a cake layer on the membrane. The optical clarity of the fluid above the cake was checked to be sure that all the particles were deposited onto the cake. Each run consisted in setting the pressure drop across the membrane, measuring the permeate volume every 2 minutes during the cake build-up on the membrane and then measuring the permeate flux when saline solution was filtered through the cake layer.

Permeate flux decreased with time and reached a steady-state value once all the yeast had accumulated in the cake on the membrane. The superficial permeation velocity is related to the variation in permeate volume according to:

$$\langle u \rangle = \frac{1}{A} \frac{dV}{dt} \quad (20)$$

Then the specific resistance of the rehydrated cells cake can be calculated from the rate of variation in permeate volume using a variant of Eq. 18:

$$\frac{dV}{dt} = \frac{A p_0}{\eta (R_m + \bar{\alpha} \cdot m)} \quad (21)$$

Here R_m is the hydraulic resistance of the clean membrane and $\bar{\alpha}$ is the experimentally determined specific resistance; it is worth noting that $\bar{\alpha}$ is an average value that includes both bed deformation effects and surface layer effects. If the average resistance $\bar{\alpha}$ is constant throughout the experiment, then Eq. 21 is valid both during the

stationary phase when the cake is completely formed (\bar{m} is then a constant) and during the initial phase of cake formation (when \bar{m} is variable).

The mass \bar{m} of rehydrated cells that has accumulated on the membrane per unit area can be calculated from the mass of dry yeast in the initial suspension C , $\bar{m} = \kappa C V / A$ where κ a proportionality constant ($\kappa = 1.8$ as determined experimentally by Starov & al., 2002) used to convert the yeast cell dry weight into the yeast cell rehydrated weight.

Substitution of the latter expression in equation (21) gives the following relationship:

$$\frac{dV}{dt} = \frac{A^2 p_0}{\eta(R_m A + \alpha \kappa C V)} \quad (22)$$

Integration of Eq. 22 gives the relationship for the transitory phase:

$$\frac{t}{V} = \frac{\eta R_m}{A p_0} + \frac{\alpha \kappa C \eta}{2 A^2 p_0} V \quad (23)$$

This is the traditional filtration equation for constant pressure filtration, very similar to Ruth's equation (Ruth, 1935). Eq. 23 was used to determine the specific resistance of yeast cakes from experimental data in the transitory phase.

Furthermore, Eq. 21 was used to calculate the value of the specific resistance during the stationary phase (i.e. when all the yeast cells have accumulated in the cake) where the mass of deposited cells is known from the initial weight of cells according to $\bar{m} = \kappa C V_f / A$ with V_f is equal to the total volume of permeate collected during the cake formation phase.

In this work the values determined from the transitory phase were found to be consistent with the steady-state values, and the latter are considered for the discussion.

3.3. *Compressibility: centrifugal measurement procedure*

The compressibility of the yeast cells was studied through a *multiple-speed equilibrium sediment height* (MSESH) technique first developed by Buscall and White (1987). This technique has been mainly used to determine in an accurate way the compression characteristics of mineral flocculated suspensions (Miller, Melant & Zukoski, 1996) or to examine consolidation mechanisms during dewatering of fine tailings (deKretser, Scales & Boger, 1997). In the MSESH technique a centrifuge is used to determine the compressive yield stress function $p_s(\phi)$, i.e. the force or pressure a network can sustain without undergoing a re-arrangement. In this approach, the compressive yield stress is assumed to be an explicit function of solid volume fraction and an implicit function of the interparticle bridging force. The latter implicit function can be determined through different experimental procedures (Miller, Melant & Zukoski, 1996). In this work, we have retained a MSESH technique that we briefly describe here.

Samples of cell suspensions of known initial volume and solids content are placed in cylindrical, transparent, flat-bottomed centrifuge tubes and the equilibrium height h_{eq} is measured for various increasing values of centrifugal acceleration at the bottom of the tube $R\omega^2 = Ng$. The initial volume fraction of the suspension is assumed to be uniform throughout the tube. Raw data required are the initial height of the suspension, the density difference between solid and liquid phases and the centrifuge radius from the center to the base of the tube.

A typical plot of $h_{eq}(Ng)$ is shown in Fig. 3. The curves are linear when plotted on semi-logarithmic coordinates. The conversion of this raw data to a $p_s(\phi)$ curve is not trivial. Buscall & White (1987), Landman, White & Buscall (1988), and Green, Eberl &

Landman (1996) after considerable work have developed a procedure to estimate such constitutive equations for compressible beds.

There are two routes to process the data: a full iterative algorithm and an approximate solution. It was shown that the approximate solution is acceptable if a limited number of data are available. The theory for these techniques is fully detailed in the above references and the basic equations for the approximate solution are given in the Appendix. As reported by Green & Boger (1997) a certain minimum centrifuge tube diameter must be used to minimize any possible wall effects, as narrow tubes may restrict the compressibility of the suspensions and generate unrealistically low results. A tube diameter of 24 mm was used for all experiments, the widest practical tube diameter for the results presented here. This does not mean that the wall effect is entirely eliminated using this tube diameter, but possible wall effects on the compressive behavior of the suspensions are minimized.

4. Results

4.1. Deformation of yeast cells under mechanical load

We have measured the compressive yield stress for different solid fractions in the range 0.5 - 0.9. It is seen in Fig. 4 that a solids fraction as high as 85% can be reached for compressive yield stress in the range of 10 to 50 kPa. These results are in good agreement with those discussed by Zydney, Saltzman & Colton (1989) for red blood cells who found a solids fraction as high as 98% for a compressive yield stress of 12 kPa. Yeast cell deformation has been observed during a slow drying process on a microscope slide through an optical microscope. Fig. 5 illustrates the deformation of

yeast cells used in our study during such a drying process: this creates a hexagonal arrangement similar to that observed by Zydney, Saltzman & Colton (1989).

4.2. *Filtration results*

We determined the specific resistance of the cake $\bar{\alpha}$ from the variation of t/V versus the permeate volume V as detailed above. The membrane resistance R_m during the experiment was obtained from the extrapolation of the data for $V = 0$. The average specific resistance of the cake $\bar{\alpha}$ could also be determined from final resistance $\bar{\alpha}m$, that is observed when all the solid material in the suspension has accumulated on the membrane. The specific resistance values measured in both ways are consistent. Specific resistance data obtained from experiments are plotted in Fig. 6 as a function of applied pressure. The $\bar{\alpha}$ values are close to the values previously measured by others. A power law is found to fit the pressure dependency, as frequently reported. This power law does have some defects: in particular it implies a zero specific resistance at zero pressure. However as it is a standard analysis technique, it has been applied in the present work. Here the compressibility index n was close to 0.8 (Fig. 7) to be compared with usual values ranging from 0 for incompressible material to 0.9 for highly flocculated compressible sludge and to compressibility index found in the literature. For rehydrated yeasts or cultivated yeasts compressibility index lying between 0.25 and 0.9 have been reported depending on the range of the applied pressure, of the composition of the suspending media and of the rinsing procedure.

5. Discussion

5.1. *Deformation of yeast cells under mechanical load*

Fig. 7 shows a comparison between the deformation of yeast cells measured using centrifugal experiments based on the MSESH technique and the model described above with the values of the parameters determined by Smith, Zhang & Thomas (2000) for Π_{c0} , r_0 , β and K . The experimental data (points) show less compression than is predicted by the model when using the published values of the parameters (the continuous curve). A first possibility to explain this, is the uncertainty in the determination of the four parameters of the model: indeed the published values have only a moderate precision. But we have tested that the behavior of the model is relatively insensitive to the values of these parameters; this is illustrated by the dotted curve in Fig. 7 which was calculated after multiplying the surface modulus K by a factor of 2.

A more likely explanation lies in the fact that the cell deformation is largely reversible. So the bed of cells initially compressed in the centrifuge may have time to expand osmotically between the time when the centrifuge is stopped and the time when the measurement is made: a matter of several minutes. As mentioned previously Smith, Zhang & Thomas (2000), found that isolated cells reached osmotic equilibrium in about 5 s. For cells incorporated into a compressed bed, the transfer of water would be slowed by the small area of contact between cells and the aqueous phase and by the low permeability of the medium. Even so, it is possible that the expansion of the bed could be rapid enough to cause the difference in compression shown in Fig. 7. Indeed, McCarthy, O'Shea, Murrau, Walsh & Foley (1999) discussed the existence of a reversible mechanism in the compression of microbial cakes through centrifugation

experiments suggesting that measurements made when the pellet has relaxed to a zero-compressive pressure state would underestimate cell compressibility.

Finally, we also mentioned that there are two ways of treating the raw data: a full iterative algorithm and the approximate solution that was used in this work. The use of the numerical procedure would certainly improve the precision of the treatment, but this improvement is unlikely to cause important differences in the results.

5.2. *Specific hydraulic resistance*

In Fig. 6, the calculated specific resistances are plotted against the filtration pressure and compared with the experimental data. As shown the calculated values are almost two orders of magnitude lower than the experimental ones. Also the calculated values show almost no variation with the pressure and at first sight this can seem surprising for a compressible cake. The model presented above does in fact predict values of α in the same range as the experimental values, but the compressive pressure in the cake would have to be quite high ($p_s \approx 0.9$ bar). It is important to note that the compressive pressure is zero at the upper cake surface: so the top layer of cells is not compressed. Then deeper into the bed of cells and closer to the membrane, the compressive pressure increases as the hydraulic pressure in the liquid declines, according to Eq. 17. The hydraulic resistance of the uppermost cells is not high enough to create a sufficient pressure drop for there to be a strong compression of the cells closer to the membrane. In this way, the overall pressure drop calculated for this system is much lower than is observed experimentally.

There is one point however that has not been included so far in our model: the effect of the first cell layer, the one that is closest to the membrane. If we consider the results of our calculations as presented so far, the liquid pressure at that point is still quite high, with very little loss in the filter cake up to that point. The cells in the first layer experience this hydraulic pressure everywhere except on the surface where they are in contact with the membrane: through that surface there is no flow and no pressure drop, so the pressure they experience there is in fact the permeate pressure. Thus the cells in the first layer experience a much higher compressive pressure than the other cells, a compressive pressure equal to the hydraulic pressure near the membrane surface $p_l(X_d)$. Also part of their contact area is on the membrane, and this part of the membrane becomes impermeable. Already Zydney, Saltzman & Colton (1989) considered a mechanism by which cells would block pores on the membrane surface, the extent of the blockage being almost independent of the compressive pressure for the red blood cells they were working with. In the present case, the yeast cells are more nearly spherical so it would not be surprising if their contact area varied with the compressive pressure.

The fraction of open membrane area ξ can be calculated as the ratio of the resistance of the clean membrane to the apparent membrane resistance:

$$\xi = \frac{R_m}{\bar{R}_m} = \frac{R_m \eta \langle u \rangle}{p_l(X_d)} \quad (24)$$

It should be noted here that because of the low resistance of the filter cake, the hydraulic pressure at the membrane is almost equal to the applied filtration pressure: $p_l(X_d) \approx p_0$. Calculations performed on the basis of Eq. 24 give values that decrease regularly with the applied pressure (Table I): so the contact area of the cells with the membrane increases with increasing pressure. This can be put in parallel with the fact

that cell-cell contact area also increases with increasing compressive pressure. For the cells in the first layer part of the cell-cell contact should be replaced by cell-membrane contact, so the area of membrane blocked by cells should be proportional to their cell-cell contact area.

The membrane area occupied by each cell in face-centered cubic packing depends on the orientation assumed by the packing. As shown in Fig. 8 for a 'hexagonal' plane lying on the membrane it would be $2\sqrt{3}a^2$ whereas for a 'square' plane it would be $4a^2$: the two values are not very different. The cell-cell contact area per cell is $12\pi(r^2 - a^2)$. So the cell-cell contact per unit membrane area is $2\sqrt{3}\pi(r^2/a^2 - 1)$ for the 'hexagonal' arrangement and $3\pi(r^2/a^2 - 1)$ for the 'square' arrangement: let us assume an intermediate value of $10(r^2/a^2 - 1)$. The ratio of this quantity to the calculated fraction of membrane area blocked by cells gives the fraction of cell-cell contact. As shown in Table 1, this fraction is independent of the compressive pressure (applied pressure) and is about 13%. This value seems reasonable to explain the major part of the cake resistance can be accounted for by membrane-blocking mechanism in which the layer of cells in contact with the membrane experiences a compressive pressure almost equal to the filtration pressure and the resulting cell-membrane contact area is simply a moderate fraction of the cell-cell contact area that the same cells would have in a uniform bed.

6. Conclusion

While there has been a large number of studies devoted to dead-end microbial filtration in recent years, most of these have focused on empirical relations between rate

of filtration and operating pressure and arrive at the conclusion that compressibility should be invoked. However no such effects have been explicitly taken into account through a particle stress balance equation in the formulation of the problem. In the present work, experimental data on filtration through yeast filter cakes have been compared with a mechanical model developed to describe the behavior of such a bed of deformable cells.

We have also explored the possibility of using a multiple speed equilibrium sediment height technique to determine a compressive yield stress function. Here the comparison between the experimental data and the mechanical model suggests that the centrifugal technique suffers from problems related to the fairly rapid relaxation of the cell bed once compression is stopped. This technique could give better results with a centrifuge optically equipped to measure sediment height during compression.

Unlike previous studies, the present work uses a mechanical model based on independent measurements to gain insight into the role of compressive pressure in packing arrangement and flow properties of the filter cake. A modeling approach based on established theories for flow in porous media and particle stress balance shows that the behavior of yeast-cell beds in terms of compressibility and hydraulic resistance can be taken into account. The results show that simply including a plausibly compressible bed is not sufficient to explain the hydraulic resistance observed. However the high compressive pressure experienced by the first layer of cells in contact with the membrane can explain the results if it is assumed that a constant fraction (around 13%) of the contact area of the cells acts to reduce the membrane area open to flow. Future work on flow through cell beds of widely varying thickness would be valuable in testing this hypothesis as well as evaluating the influence of membrane porosity and cell

surface properties one factor not discussed in this work but also known to change the compressibility of cells.

7. Appendix

Beginning with a force balance on a differential element of the cell bed in the tube as depicted in Fig. 9, and continuity equations on the solid and liquid phases, the underlying differential equation relating the compressive yield stress P at equilibrium to the acceleration may be determined:

$$\frac{dp_s}{dr} = (\rho_c - \rho_l)\phi r\omega^2 \quad (\text{A.1})$$

Where p_s is the compressive pressure on the solid in the differential element of the bed.

Noting $r = R - x$ with $\gamma = Ng = R\omega^2$, yields

$$\frac{dp_s}{dx} = -\gamma(\rho_c - \rho_l)\phi(x)\left(1 - \frac{x}{R}\right) \quad (\text{A.2})$$

Buscall & White (1987) suggest applying this general equation (A.2) to the particular case of $x = 0$, i.e. at the bottom of the tube as detailed below. A function $X(x)$ is defined:

$$X = \int_x^{h_{eq}} \left(1 - \frac{x}{R}\right) dx = (h_{eq} - x)\left(1 - \frac{h_{eq} + x}{2R}\right) \quad (\text{A.3})$$

Equation (A.2) can then be written as:

$$\frac{dp_s}{\phi} = \Delta\rho\gamma dX \quad (\text{A.4})$$

and integrated to yield:

$$\int_0^{p_s(x)} \frac{dp_s}{\phi(p_s)} = \Delta\rho\gamma X(x) \quad (\text{A.5})$$

In particular at $x = 0$, equation (A.5) becomes:

$$\int_0^{p_s(0)} \frac{dp_s}{\phi(p_s)} = \Delta\rho \gamma X(0) \quad (\text{A.6})$$

Differentiating (A.6) with respect to γ , we obtain

$$\phi(0) = \frac{dp_s(0)}{d\gamma} \left/ \left[\Delta\rho \left(X(0) + \gamma \frac{dX(0)}{d\gamma} \right) \right] \right. \quad (\text{A.7})$$

From equation (A.6), we can also put:

$$\phi(x) = \frac{1}{\Delta\rho \gamma} \frac{dp_s}{dX} \quad (\text{A.8})$$

The mass balance $\int_0^{h_{eq}} \phi \, dx = \phi_0 h_0$ can therefore be written as:

$$\int_0^{h_{eq}} \frac{dp_s}{dX} \, dx = \Delta\rho \gamma \phi_0 h_0 \quad (\text{A.9})$$

Integrating this equation by parts we obtain:

$$p_s(0) = \Delta\rho \gamma \phi_0 h_0 - \Lambda(\gamma) \quad (\text{A.10})$$

with:

$$\Lambda(\gamma) = \frac{1}{R} \int_0^{H_{eq}} \frac{p_s(x)}{(1-x/R)^2} \, dx \quad (\text{A.11})$$

Differentiating equation (A.10) with respect to γ , we obtain:

$$\frac{dp_s(0)}{d\gamma} = \Delta\rho\phi_0 h_0 - \frac{d\Lambda}{d\gamma} \quad (\text{A.12})$$

Substituting this result in equation (A.7), we obtain:

$$\phi(0) = \left(\phi_0 h_0 - \frac{1}{\Delta\rho} \frac{d\Lambda}{d\gamma} \right) / \left(X(0) + \gamma \frac{dX(0)}{d\gamma} \right) \quad (\text{A.13})$$

Equations (A.11) and (A.13) provide a way of determining the compressive pressure $p_s(0)$ and the volume fraction $\phi(0)$ at the bottom of the tube from the quantity Λ .

Buscall & White (1987) suggested an approximate solution to equations (A.10) and (A.13). It allows the compressive pressure and the volume fraction at the bottom of the tube to be calculated from the variation in the steady-state pellet height as a function of centrifugal acceleration:

$$p_s(0) \approx \Delta\rho\phi_0 h_0 \gamma \left(1 - \frac{h_{eq}}{2R} \right) \quad (\text{A.14})$$

$$\phi(0) \approx \frac{\phi_0 h_0 \left[1 - \frac{1}{2R} \left(h_{eq} + \gamma \frac{dh_{eq}}{d\gamma} \right) \right]}{\left(h_{eq} + \gamma \frac{dh_{eq}}{d\gamma} \right) \left(1 - \frac{h_{eq}}{R} \right) + \frac{h_{eq}^2}{2R}} \quad (\text{A.15})$$

For a set of initial volume fractions ϕ_0 and volumes h_0 in the tube, we have determined the variation of h_{eq} with centrifuge acceleration γ as shown in Fig. 8. The quantity $dh_{eq}/d\gamma$ is therefore defined as the slope of that curve for a given set of data.

Green, Eberl & Landman (1996) have shown that this variation of h_{eq} with γ when normalized with respect to initial conditions $h_0 \phi_0$ follows a polynomial law.

Here the best adjustment is obtained with a polynomial function of the type:

$$\ln\left(\frac{h_{eq}}{h_0 \phi_0}\right) = a_0 + a_1 \ln \gamma + a_2 (\ln \gamma)^2 + a_3 (\ln \gamma)^3 \quad (\text{A.16})$$

with $a_0 = -0.671$; $a_1 = 0.427$; $a_2 = -4.68 \times 10^{-2}$; $a_3 = 1.39 \times 10^{-3}$

Applying equation (A.16) to each set of data (h_{eq}, γ) , we could estimate the variation of $dh_{eq}/d\gamma$ for a large range of initial conditions (ϕ_0, h_0) .

8. References

Buscall, R. & White, L.R. (1987). The consolidation of concentrated suspensions. *J. Chem. Soc. Faraday Trans. I.*, 83, 873-891.

Dullien, F.A.L. (1979). *Porous Media: Fluid Transport and Pore Structure*. New York: Academic Press.

Green, M.D., Eberl, M., & Landman, K.A. (1996). Compressive yield stress of flocculated suspensions: determination via experiment. *AIChE J.*, 42, (8), 2308

Green, M.D., & Boger, D.V. (1997). Yielding of suspensions in compression. *Ind. Eng. Chem. Res.*, 36, 4984-4992.

DeKretser, R.G, Scales, P.J., & Boger, D.V. (1997). Improving clay-based tailing disposal: a case study on coal tailings. *AIChE J.*, 43, 1894-1903.

Landman, K.A., White, L.R., & Buscall, R. (1988). The continuous-flow gravity in thickener: steady state behavior, *AIChE J.*, 34, 239.

McCarthy A.A, Gilboy P.,Walsh P.K.,& Foley G.(1999), Characterisation of cake compressibility in dead-end microfiltration of microbial suspensions, *Chem. Eng. Com*, 173, 79-90.

Meireles, M., Clifton, M.J., & Aimar, P. (2002). Filtration of yeast suspensions: experimental observations and modelling of dead-end filtration with a compressible cake. *Desalination*, 147, 19-23.

Miller, K.T., Melant, R.M., & Zukoski, C.F. (1996). Comparison of compressive yield response of aggregated suspensions: pressure filtration, centrifugation and osmotic consolidation. *J. Ceram. Soc.*, 79(10), 2545-2564

Nakanishi, K., Tadokoro, T., & Matsuno, R. (1987). On the specific resistance of cakes of microorganisms. *Chem. Eng. Comm.*, 62, 187-201.

Nomura, S. (1989). Studies on filtration mechanism in cross-flow microfiltration. Master's Thesis, Chem. Eng., University of Tokyo

Ogden, G.E., & Davis, R.H. (1990). Experimental determination of the permeability and relative viscosity for fine latexes and yeast suspensions. *Chem. Eng. Comm.*, 91, 11-28.

Ofsthun, N.J. (1989). Crossflow membrane filtration of cell suspensions. Ph. D. Thesis, Massachusetts Institute of Technology, Cambridge, Ma.

Piron, E., René, F., & Latrille, E. (1995). A cross flow filtration model based on integration of the mass transport equation. *J. Membr. Sci.*, 108, 57-70.

Redkar, S.G., & Davis, R.H. (1993). Crossflow microfiltration of yeast suspensions in tubular filters. *Biotechnol. Prog.* 9, 625-634.

Rushton, A., & Khoo, E. (1977). The filtration characteristics of yeast. *J. Appl. Chem. Biotechnol.*, 27, 99-109.

Ruth B.F.(1935) .Studies in filtration.III.Derivation of general filtration equations, *Ind.Eng. Chem*, 27, 708-715.

Smith, A.E., Zhang, Z., & Thomas, C.R. (2000). Wall material properties of yeast cells: Part 1. Cell measurements and compression experiments. *Chemical Engineering Science*, 55, 2031-2041.

Smith, A.E., Moxham, K.E. & Middelberg, A.P.J. (1998). On uniquely determining cell-wall material properties with the compression experiment. *Chemical Engineering Science*, 53, 3913-3922.

Smith, A.E., Moxham, K.E. & Middelberg, A.P.J. (2000). Wall material properties of yeast cells: Part 2. Analysis. *Chemical Engineering Science*, 55, 2043-2053.

Sorensen, P.B., Moldrup, P., Hansen, J.A.A. (1996). Filtration and expression of compressible cakes. *Chemical Engineering Science*, 51(6), 967-979.

Starov, V., Zhdanov, V., Meireles, M., & Molle, C. (2001). Viscosity of concentrated suspensions: influence of cluster formation. *Advances in Colloid and Interface Science*, 96, 279-293.

Succi, S. (2001). *The Lattice Boltzmann Equation for Fluid Dynamics and Beyond*, Oxford: Clarendon Press.

Tiller, F.M. (1975). Compressible cake filtration. In K.J. Ives, *The Scientific Basis of Filtration*, Leyden: Noordhoff.

Tiller, F.M., Yeh, C., & Leu, W.F. (1987). Compressibility of particulate structures in relation to thickening, filtration and expression, a review. *Sep. Sci. Technol.*, 22, 1037-

Zydney, A.L, Saltzman, W.M., & Colton, C.K. (1989). Hydraulic resistance of red cell beds in an unstirred filtration cell. *Chem. Eng. Sci.*, 44, 147-159.

9. Notation

A	membrane area (m^2)
a	half-distance between centers of two neighboring cells (m)
C	concentration of dry solid in the suspension (kg m^{-3})
g	acceleration due to gravity (m s^{-2})
h_0	initial sediment height (m)
h_{eq}	equilibrium sediment height (m)
K	surface modulus (N m^{-1})
K_0	Kozeny coefficient (-)
m	mass of rehydrated cells cake per membrane area (kg m^{-2})
n	compressibility index
N	gravity number
p	hydrostatic pressure (Pa)
p_0	applied filtration pressure (Pa)
p_s	compressive pressure on solid phase (Pa)
r	radius of curvature, radial distance (m)
r_h	hydraulic resistivity (m^{-2})
R	radius of the centrifuge rotor (m)
R_m	membrane resistance (m^{-1})
\bar{R}_m	apparent membrane resistance (m^{-1})
S	surface area per unit volume (m^{-1})
S_c	surface area per cell (m^2)
T	membrane tension (Pa)
t	time (s)
$\langle u \rangle$	superficial liquid velocity in porous medium (m s^{-1})

V	permeate volume (m^3)
V_c	volume of a cell (m^3)
X_d	cake thickness (m)
x	space coordinate (m)

Greek symbols

α	specific resistance per mass of wet cake (m kg^{-1})
$\bar{\alpha}$	average specific resistance per mass of wet cake (m kg^{-1})
β	non-osmotic fraction of cell volume (-)
Δ	difference between inside and outside of cell
κ	coefficient to convert dry cell weight into rehydrated cell weight
η	viscosity (Pa s)
ξ	fraction of membrane blocked by cells (-)
Π	osmotic pressure (Pa)
ρ	density (kg m^{-3})
ϕ	volume fraction of solid (-)
ω	angular velocity (rad s^{-1})

Subscripts

c	cell, cell interior
l	liquid phase
s	solid phase
0	value at zero cell membrane tension, value at $x = 0$
'	value for uncompressed cell

10. Figure Captions

Fig. 1. Specific resistance of yeast cakes as a function of operating pressure. Data from Piron, René & Latrille (1995), Nomura et al. (1984), Nakanishi et al. (1987), Rushton et al. (1977). Shown for comparison is the resistance calculated using the Carman-Kozeny equation (Eq. 14) with a cell density ρ_c of 1130 kg/m³, a cell diameter of 5 μ m and a solids volume fraction of 0.74.

Fig. 2. Flow diagram showing how Equations 3 and 6- 15 can be used to determine hydraulic resistivity and solid cake fraction.

Fig. 3. Typical raw data generated by multiple-speed equilibrium sediment height technique for the determination of compressive yield stress.

Fig. 4. Deformation of yeast cells under mechanical load from MESH values experiments. Compressive pressure as a function of volume fraction of solids for pellets formed from rehydrated yeasts .

Fig. 5. Micrograph of a yeast suspension during a slow drying process. Cells are deformed by flattening in regions of cell-cell contact while remaining rounded elsewhere.

Fig. 6. Specific resistance of a bed formed from washed rehydrated yeasts as a function of pressure. Black dots are experimental data and white dots calculated values

Fig. 7. Deformation of yeast cells under mechanical load. Black dots are experimental MESH values, the continuous curve shows the prediction of the mechanical model with standard values for the yeast properties and the dashed curve is from the model with the membrane surface modulus K multiplied by 2.

Fig. 8. Schematic representation of cell-cell contact area near the membrane.

Fig. 9. Raw data curve fitting with a third-order polynomial law.

11. Tables

Table I. Calculated values of the fraction of membrane area blocked by cells from the ratio of clean membrane resistance to apparent membrane resistance (Eq. 24).

Table I

p_0	(kPa)	50	50	75	100	150	200
$R_m \times 10^{-12}$	(m^{-1})	1.93	2.40	2.40	2.40	2.40	2.06
$\langle u \rangle \times 10^6$	(m/s)	18.0	16.0	23.3	30.2	44.2	56.0
\bar{m}	($g\ m^{-2}$)	49.4	60.0	58.0	50.2	56.5	60.0
$\bar{\alpha} \times 10^{-12}$	(m/kg)	10.4	11.3	13.1	14.7	17.4	25.6
$\alpha \times 10^{-12}$	(m/kg)	0.167	0.169	0.172	0.174	0.184	0.191
$1 - \xi$		0.300	0.226	0.248	0.270	0.287	0.419
Cell-cell contact area per unit membrane area		1.63	1.63	2.03	2.37	2.96	3.47
Fraction of cell-cell contact area blocking the membrane (%)		18.4	13.8	12.2	11.4	9.7	12.1

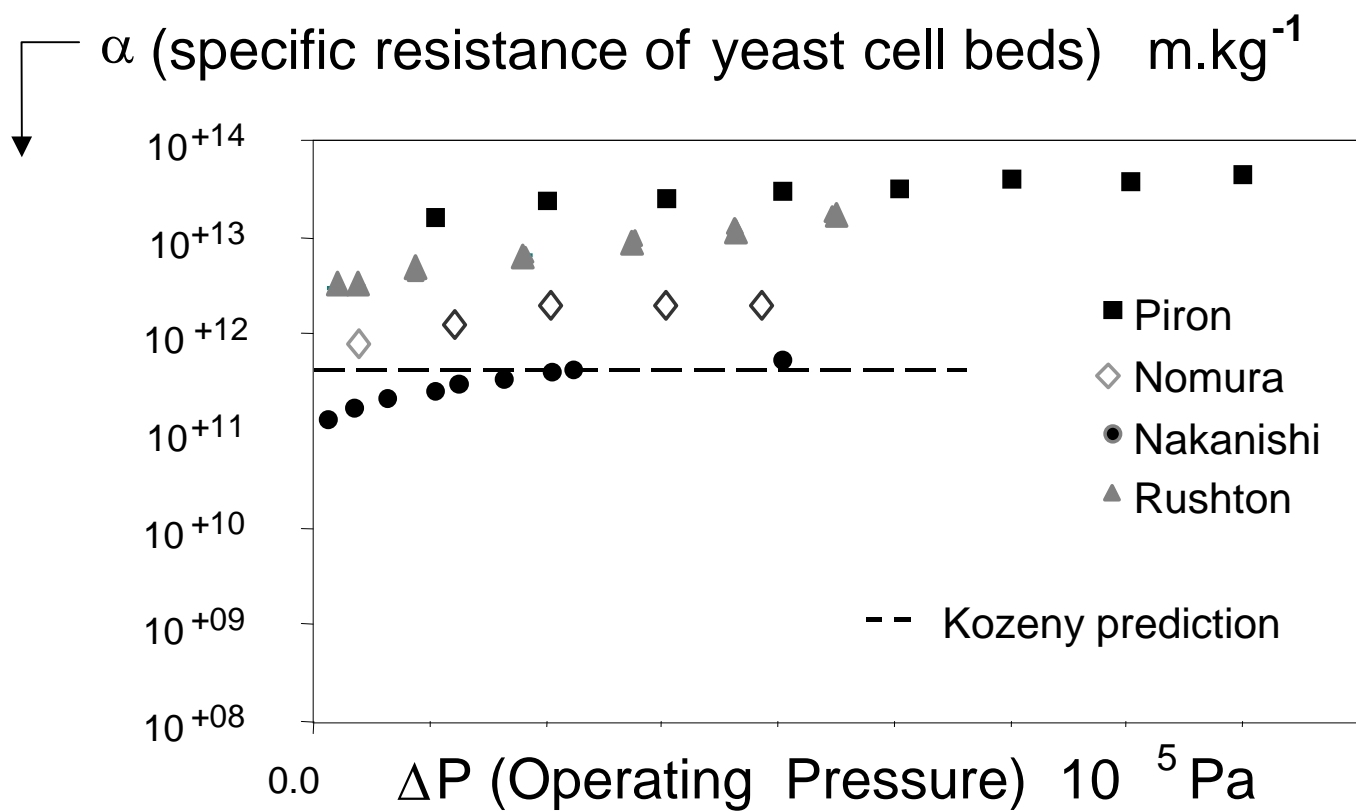


Figure 1

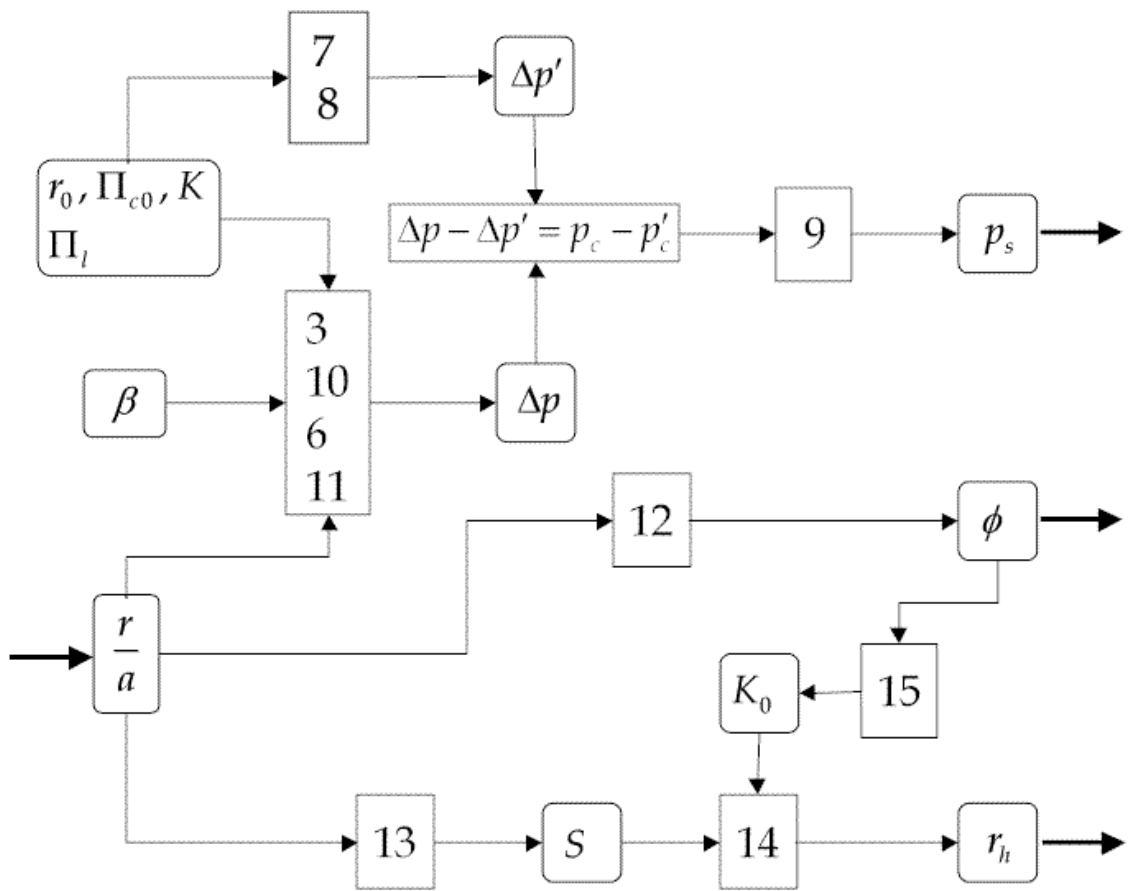


Figure 2

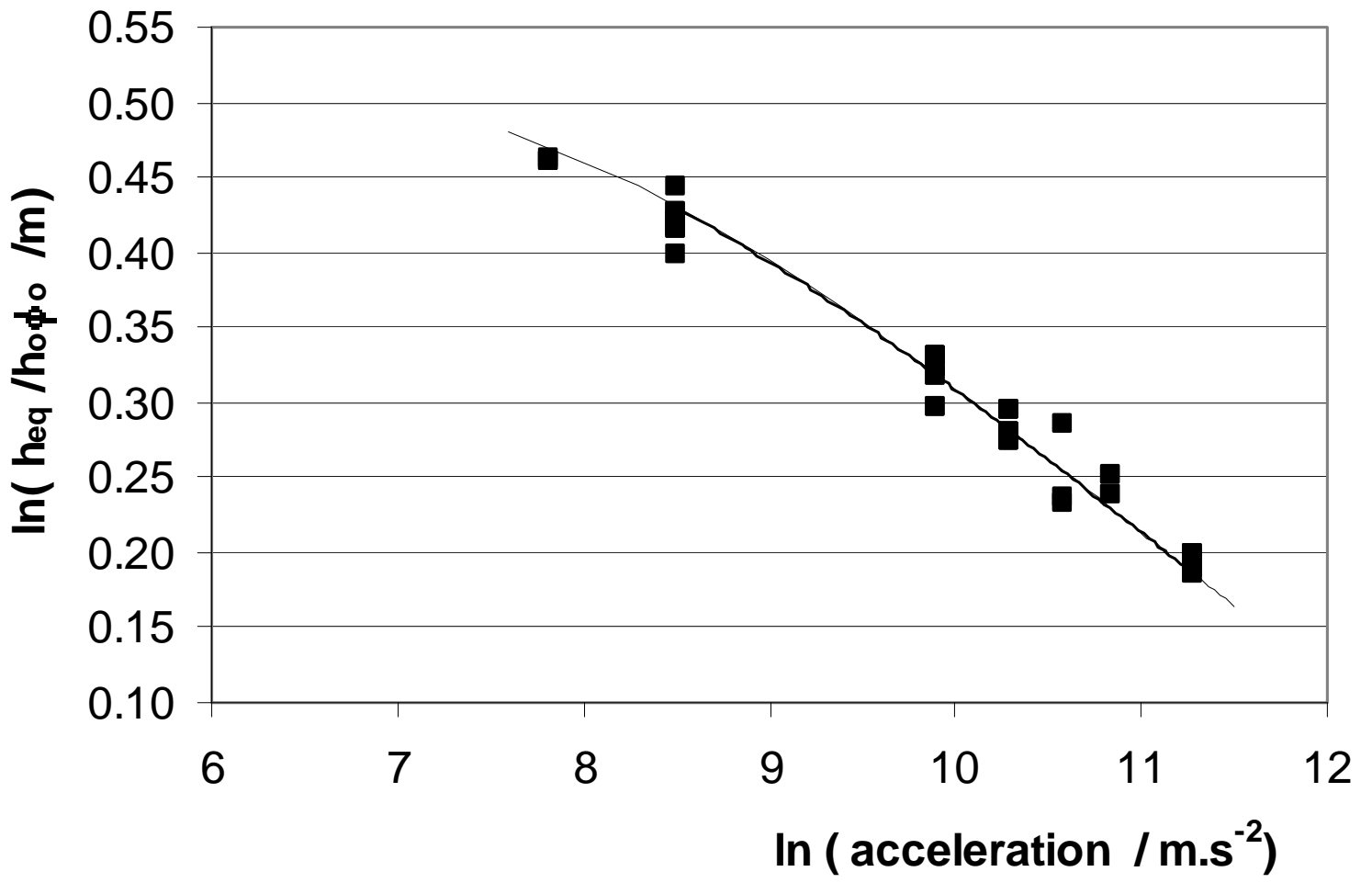


Figure 3

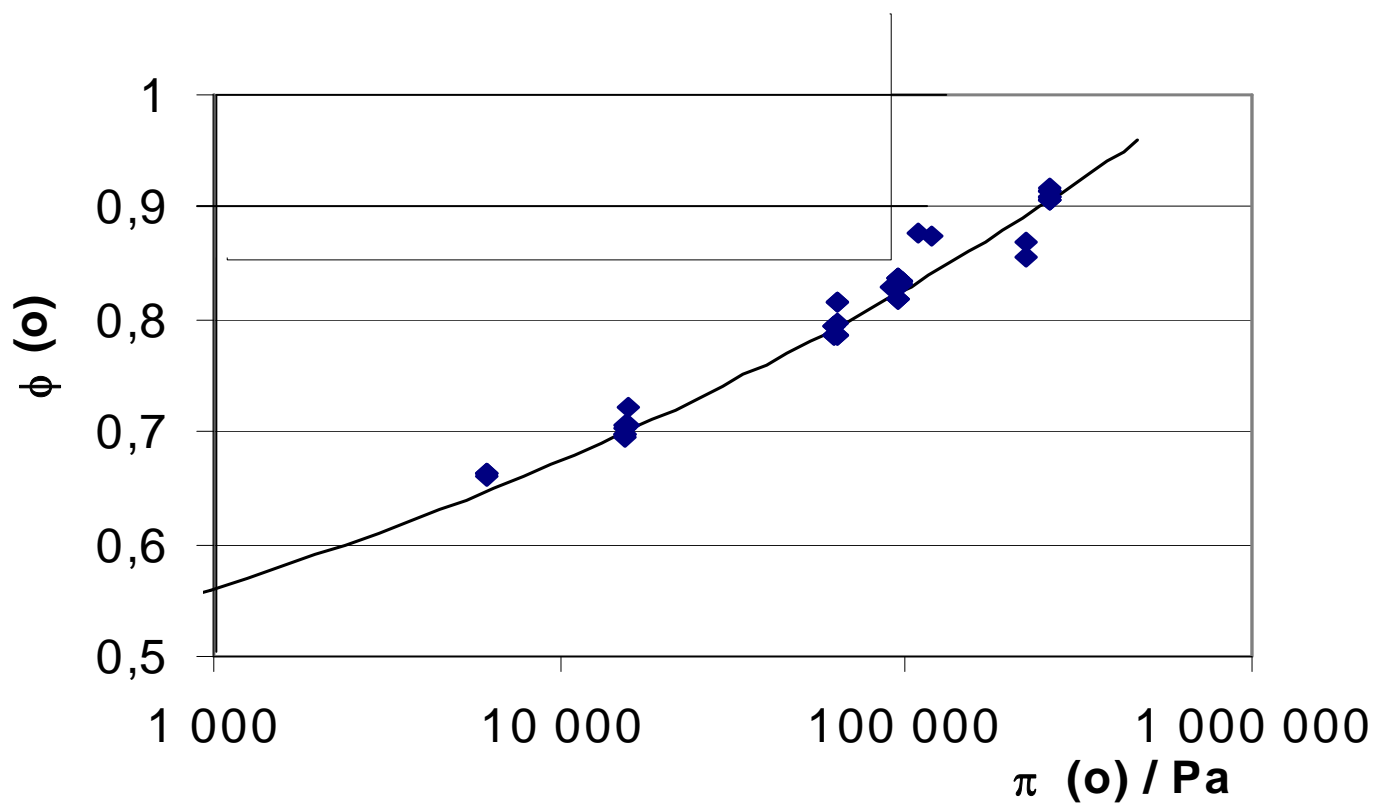


Figure 4

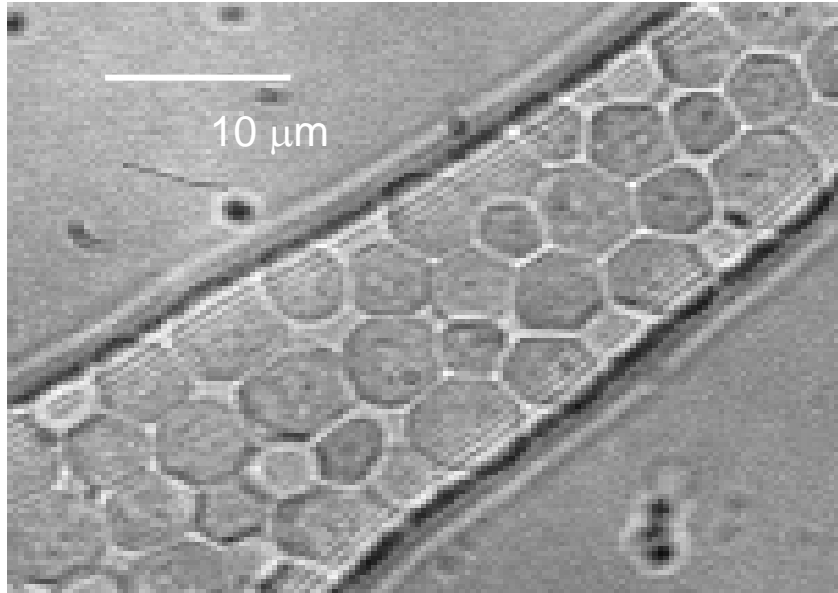


Figure 5

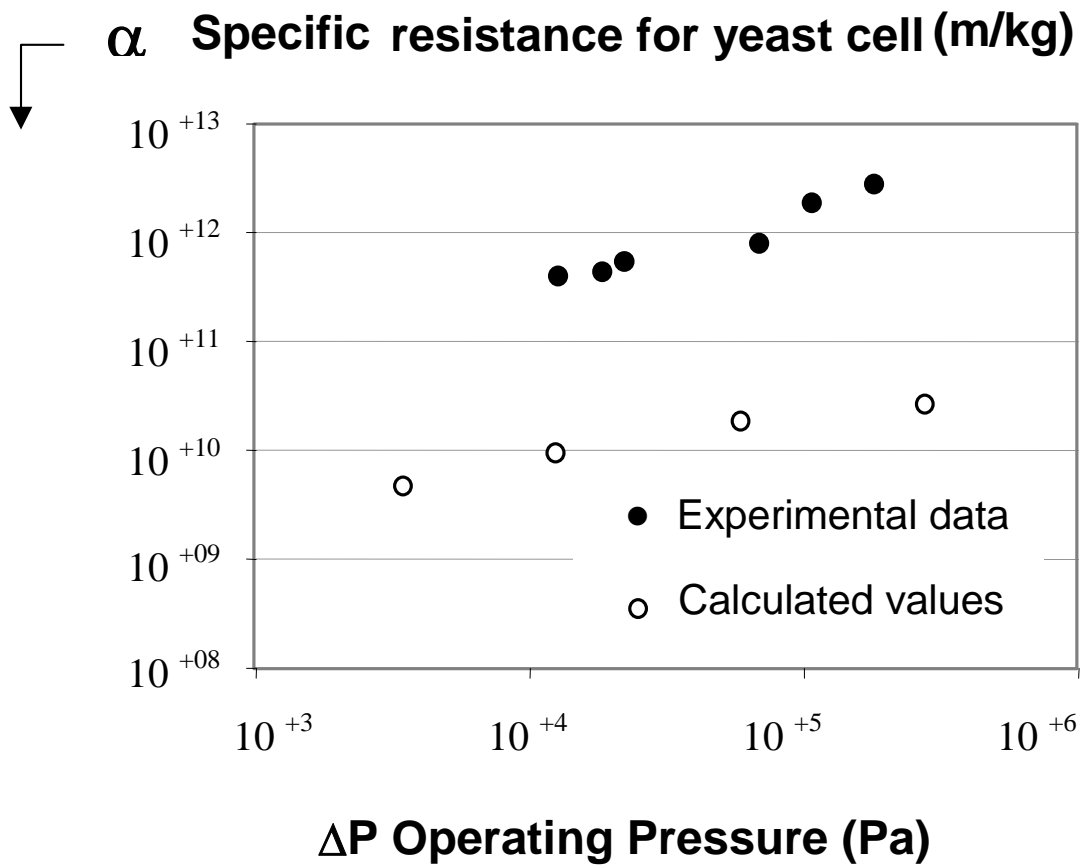


Figure 6

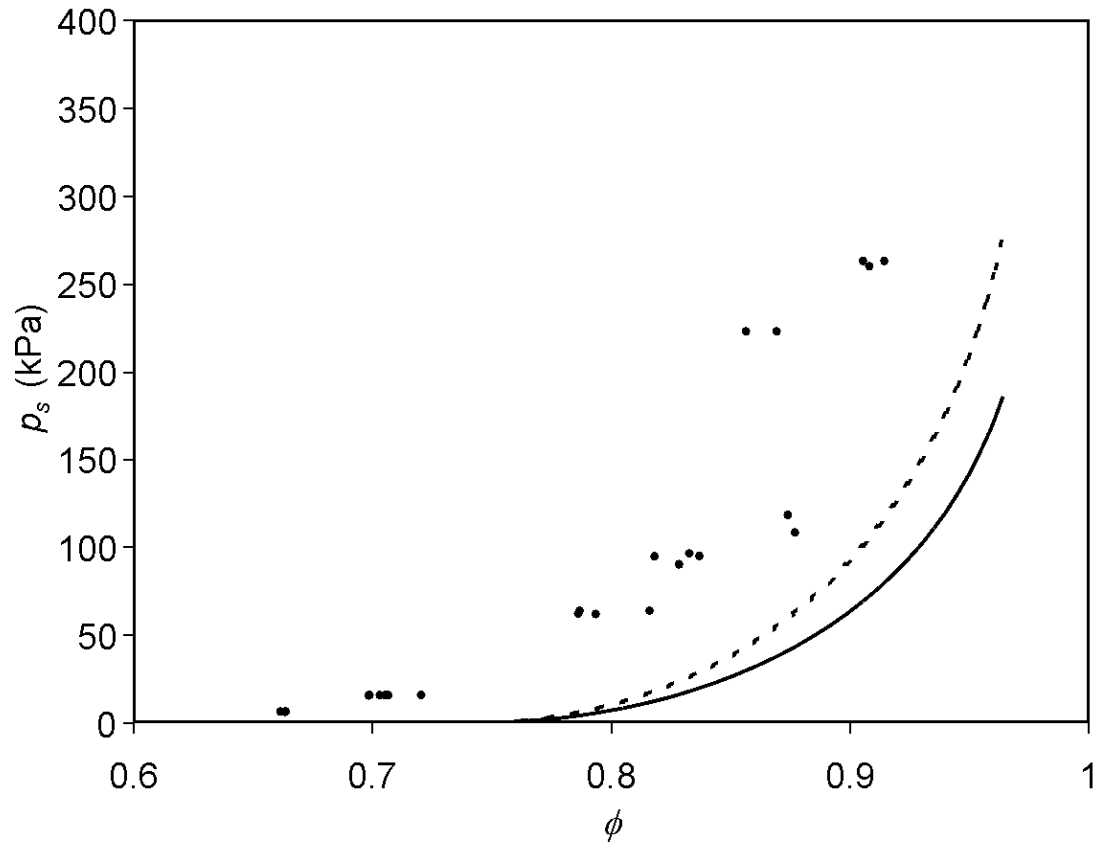


Figure 7

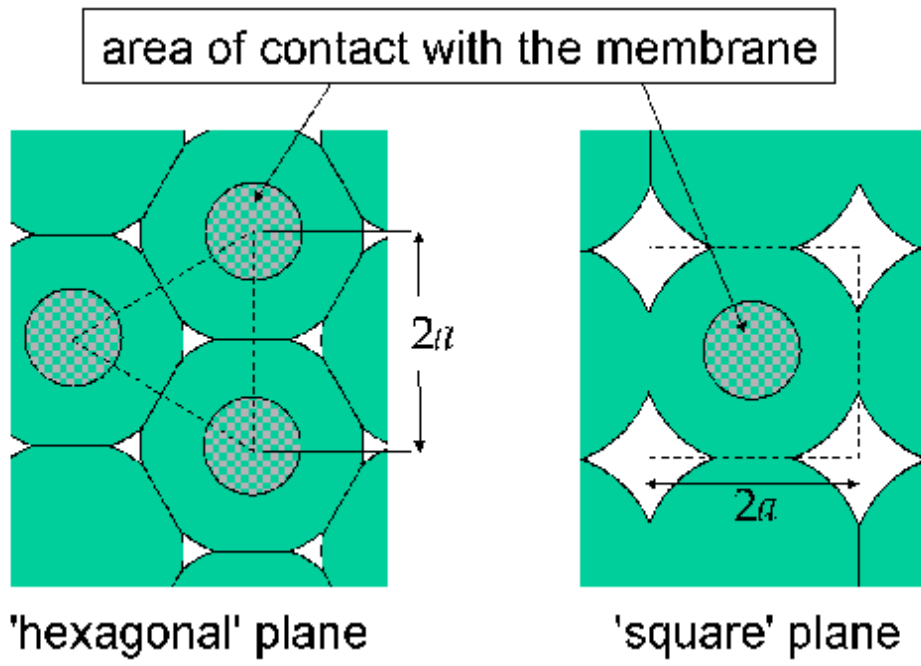


Figure 8

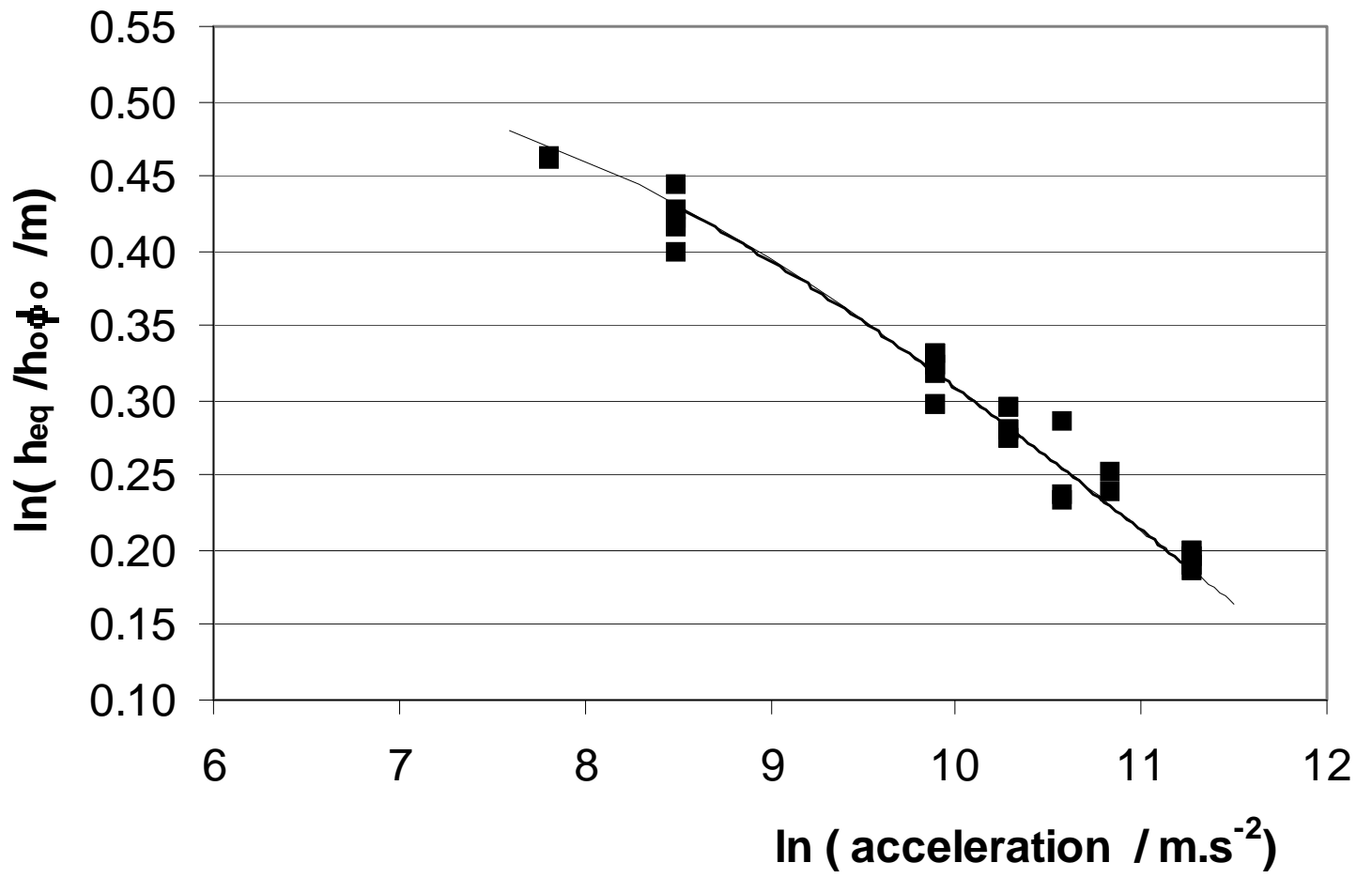


Figure 9